PACS numbers: 42.65.Hw; 42.62.Cf; 42.60.By
DOI: 10.1070/QE2000v030n05ABEH001720

Numerical analysis of subsonic laser-supported combustion waves

S T Surzhikov

Abstract. A nonstationary model of radiation gas dynamics for subsonic laser-supported combustion waves is presented. A systematic numerical simulation of the temperature and gas-dynamic structure of such waves under the conditions of experiments of E L Klosterman and S R Byron is carried out. It is shown that the dominant process governing the propagation of subsonic laser-supported combustion waves in this case is the reabsorption of heat radiation ahead of the wave front, whereas the gas-dynamic processes are of minor importance.

1. Introduction

The subsonic propagation of a plasma toward a laser beam has been discovered in 1969 in the experiments [1], where a laser spark in air induced by focused radiation of a millisecond neodymium laser was studied. The propagation of plasma was observed during ~ 1 ms at the laser radiation intensity $W \sim 8 - 15$ MW cm^{-2}. The diameter of a focal laser spot d formed by a lens with focal distance $f =$ 50 cm was $\sim 0.25 - 0.35$ mm. The velocities of plasma propagation along the beam had substantially subsonic values of $\sim 10 - 30$ m s^{-1}. The phenomenon observed in the experiments was interpreted by the authors to be an analogue of slow-combustion waves. A detailed review of the theoretical and experimental results obtained by the authors of this discovery in 1969 – 88 is given in Ref. [2].

In Refs [3 – 5], the possibility of subsonic plasma propagation in a CO_2 laser beam and, in particular, the possibility of a continuous optical discharge (COD) in a focused laser beam were theoretically substantiated and experimentally proved.

The works cited above inspired a long series of experimental and theoretical investigations in which subsonic laser-supported combustion waves (SLSCWs) were thoroughly studied. This paper is devoted to the analysis of the velocity of wave propagation along a laser beam, which is one of the main characteristics of this phenomenon. Because of this, we mention only those papers among hundreds of papers devoted to the study of laser-supported combustion waves and their applications where this question was directly discussed.

As early as in the first paper on SLSCWs [1], the authors draw attention to a noticeable disagreement between their velocities measured in the experiment and the velocities calculated within the framework of the one-dimensional theory of 'combustion starting from a closed end' [6]. A similar disagreement was observed in Ref. [5]. An important specific feature of these papers [1, 5] is that the theoretical models were constructed under the assumption that molecular heat conduction was the dominant mechanisms of heating cold gas layers ahead of the SLSCW front. Later on, the validity of this assumption was corroborated many times for SLSCWs travelling in laser beams of a small transverse size (with diameter of no greater than 1 – 2 mm). In Ref. [7], the model was constructed that explained the aforementioned disagreement. However, a considerable disagreement between the experimental and the calculated data was also observed in laser beams of considerably larger diameters.

In 1974, the results of experiments [8] on the measurement of SLSCW velocity in a CO_2 laser beam were published, where the laser beam diameter d was varied in a wide range from 0.5 to 2.1 cm. In the theoretical paper [9], which appeared immediately after [8], the one-dimensional radiation model of SLSCWs was first formulated and realised. In this model, in contrast to the heat conduction model [1, 5], a cold gas ahead of the SLSCW front is heated by the heat emission of a laser-produced plasma itself. For the transverse laser beam sizes studies in Ref. [8], this assumption was found to be well substantiated. However, even the radiation model was unable to describe the experimental data with a sufficiently high accuracy. The SLSCW velocity predicted by the theory was understated by a factor of about three (Fig. 1).

In 1971, R Conrad performed experiments to analyse the SLSCW velocity in the radiation-supported regime, which are likely to be the first experiments concerning this problem (unfortunately, the results were published only in a report; for detail, see Ref. [10]). However, these experiments were performed under different conditions than those used in Ref. [8]. The SLSCW was stabilised by the counterpropagating flow of a gas (N_2). The laser beam diameter at the SLSCW stabilisation point was about 3.2 cm. The gas flow velocity was close to 10 m s^{-1}, and the laser radiation intensity was about ~ 18 kW cm^{-2}.

Thus, by the mid-70s, a large number of experimental data on the SLSCW velocity in the regimes supported by heat conductivity and radiation were obtained. In further calculation and theoretical studies, a considerable progress in the numerical description of this process was achieved:

(1) One-dimensional and quasi-two-dimensional models of radiation gas dynamics (RGD) were developed, which made it possible to obtain a good agreement of their results with the experimental data on limiting values of gas flow

S T Surzhikov Institute for Problems of Mechanics, Russian Academy of Sciences, pr. Vernadskoro 101, 117526 Moscow, Russia

Received 11 November 1999
Kvantovaya Elektronika **30** (5) 416 – 420 (2000)
Translated by A N Kirkin, edited by M N Sapozhnikov

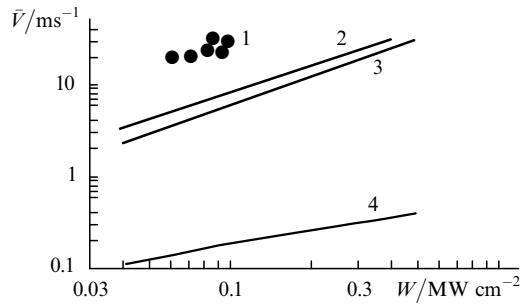

Figure 1. Comparison of the experimental and calculated average velocities obtained for laser-supported combustion waves by using different calculation models [9]. (1) Experimental data [8] for a laser beam 21 mm in diameter; (2) upper limit determined by the one-dimensional model [9]; (3) self-consistent solution [9] taking into account the radiative heat exchange; (4) heat conduction model without the radiative heat-exchange [5].

velocity in a continuous optical discharge of a small transverse size (in the heat conduction regime) [11 – 13];

(2) a completely two-dimensional RGD model was proposed [14];

(3) on the basis of the stationary RGD model [15], the radiation-supported regime of propagation of SLSCWs was studied [7]; the calculations showed that it was of principal importance to take the two-dimensional gas-dynamic effects into account (note that this fact was mentioned by the authors of first works on SLSCW [2]);

(4) in a series of papers [16 – 18], characteristics of laser-supported combustion waves formed near a target were thoroughly studied, which made it possible to understand in greater detail the initial phase of the process going on in many experiments.

The development of a completely nonstationary RGD model [19] provided a change to a qualitatively new stage of numerical study of SLSCWs, namely, the description of nonstationary RGD process on the basis of Navier – Stokes equations. The initial phase of formation of SLSCWs was studied in Ref. [20]. In particular, a steady-state gas-dynamic structure was shown to be formed in the neighbourhood of these waves for about 100 ms, which agrees well with the experiments of R Conrad [10], but casts doubts on the adequacy of the results obtained by using the quasi-stationary calculation model [14, 15] to the results on SLSCW propagation obtained in the experiments [8], where this process was observed for ~ 3 ms.

In this paper, the nonstationary RGD model [19, 20] is used to interpret the experimental data [8].

2. Statement of the problem and the calculation method

We consider the nonstationary propagation of SLSCWs in the laser radiation field and the gravity field near a surface upon the formation of an initiating plasma region and the departure of a shock wave, which is formed at the initial moment, by a considerable distance from a region under study. The problem is solved in the two-dimensional cylindrical geometry, which corresponds to the symmetry conditions of the process under study. The radiation beam of a 10.6-μm CO_2 laser is incident on a plasma from above, which corresponds to the experimental conditions [8]. A gas is assumed to be initially motionless, the pressure is constant at all points of the region where calculations are carried out, and the initial temperature distribution is quasi-Gaussian, with the maximum temperature at the centre $T_m = 18$ kK and the temperature at the periphery $T_\infty = 300$ K. The problem was solved to study the evolution of the initial plasma formed in SLSCWs and its propagation towards the laser beam.

The thermodynamic state of a low-temperature plasma is described in the LTE (local thermodynamic equilibrium) approximation. Its use can be substantiated by two facts. First, the previously developed calculation models [7, 9 – 13, 16 – 18] based on the LTE model allowed us to obtain a good agreement of the results on laser-produced plasma dynamics with the experimental data. Second, in Ref. [21], where the kinetic two-temperature model of hydrogen plasma under conditions close to those analysed in the present paper was studied, a conclusion was made that the deviation from LTE has only an insignificant effect on the dynamics of SLSCWs. However, it should be noted that the effect of models describing the thermodynamic state of laser-produced plasma in air on the dynamics of SLSCWs remains an open question and calls for a further study.

The dynamics of SLSCWs is analysed by using the following system of continuity equation, Navier – Stokes equation, energy conservation equation, and radiative transfer equations for laser and selective heat radiation in the multigroup approximation:

$$\frac{\partial \rho}{\partial t} + \operatorname{div}(\rho \boldsymbol{V}) = 0, \tag{1}$$

$$\frac{\partial \rho u}{\partial t} + \operatorname{div}(\rho u \boldsymbol{V}) = -\frac{\partial p}{\partial x} + S_u - g\rho, \tag{2}$$

$$\frac{\partial \rho v}{\partial t} + \operatorname{div}(\rho v \boldsymbol{V}) = -\frac{\partial p}{\partial r} + S_v, \tag{3}$$

$$\rho c_p \frac{\partial T}{\partial t} + \rho c_p \boldsymbol{V} \operatorname{grad} T = \operatorname{div}(\lambda \operatorname{grad} T) - Q_R + Q_L, \tag{4}$$

$$Q_L = \chi_\omega(x, r=0) P_L \exp\left(-\frac{r^n}{R_L^n}\right) \times \exp\left[-\int_0^x \chi_\omega(x', r=0)\mathrm{d}x'\right] \frac{1}{\pi R_L^2}, \tag{5}$$

$$Q_R = \sum_{k=1}^{N_k} k_k (U_{b,k} - U_k) \Delta\omega_k, \tag{6}$$

$$\operatorname{div}\left(\frac{1}{3k_k} \operatorname{grad} U_k\right) = -k_k(U_{b,k} - U_k), \quad k = 1, 2, \ldots, N_k, \tag{7}$$

where

$$S_u = -\frac{2}{3}\frac{\partial}{\partial x}(\mu \operatorname{div} \boldsymbol{V}) + \frac{1}{r}\frac{\partial}{\partial r}\left[r\mu\left(\frac{\partial u}{\partial r} + \frac{\partial v}{\partial x}\right)\right] + 2\frac{\partial}{\partial x}\left(\mu \frac{\partial u}{\partial x}\right); \tag{8}$$

$$S_v = -\frac{2}{3}\frac{\partial}{\partial r}(\mu \operatorname{div} \boldsymbol{V}) + \frac{\partial}{\partial x}\left[\mu\left(\frac{\partial u}{\partial r} + \frac{\partial v}{\partial x}\right)\right] + 2\frac{\partial}{\partial r}\left(\mu \frac{\partial v}{\partial r}\right) + 2\mu\frac{\partial}{\partial r}\left(\frac{v}{r}\right); \tag{9}$$

x and r are the axial and radial variables; ρ, c_p, and T are the density, specific heat at a constant pressure, and temperature of a gas; u and v are the axial and radial components of the velocity $\boldsymbol{V}$; p is the gas pressure; g is the acceleration of gravity; μ and λ are the coefficient of dynamic viscosity and the heat conduction coefficient of a gas; Q_{R} and Q_{L} are the volume powers of energy release associated with transfer of selective heat radiation and laser radiation; k, U, and U_{b} are the volume absorption coefficient for heat radiation and the radiative energy densities of a medium and a black body; χ_ω is the absorption coefficient for laser radiation; P_{L} is the laser power, R_{L} is the coordinate of a conventional radial boundary of laser radiation; and n is the factor characterising the intensity distribution in the cross section. The subscripts ω and k specify the spectral and group characteristics, which are determined by averaging the corresponding spectral characteristics in each of the N_k spectral ranges of wave numbers $\Delta\omega_k$.

The heat release caused by absorption of laser radiation in a low-temperature plasma of an optical discharge is calculated in the geometrical optics approximation, and the radiative transfer equation for selective heat radiation is integrated in the form of the multigroup P_1 approximation of the method of spherical harmonics. To find the power of energy release associated with heat radiation transfer, one should solve system of N_k equations (7) by using its own function $k_k(T, p)$ for each spectral range $\Delta\omega_k$.

The fact that the process under study develops at a nearly constant pressure substantially complicates the numerical solution of the problem of gas motion because the pressure drops in the system are lower than the background atmospheric pressure by several hundreds times, but, on the other hand, it substantially simplifies the problem and allows one to take into account only the temperature dependence of heat, transfer, and optical properties. In other words, one may calculate the temperature dependences of the functions listed above (ρ, c_p, μ, λ, χ, k_k) only for the atmospheric pressure and then use interpolation with respect to temperature. However, to solve the problem, one should know the temperature dependence of these properties in sufficient detail because they vary in the temperature range under study by several orders of magnitude, so that their change on one step of a finite-difference mesh may be also considerable.

We used the following boundary conditions: a heat-insulated surface, the conditions of attachment to the surface, the axial symmetry of the functions T, u, v, and U_k; and at the outer boundary of the region being calculated ($r \to \infty$ and $x \to \infty$), the boundary conditions of second kind were specified. The distances to the outer boundaries of the region were chosen so that the effect of the boundary conditions on the process under study was weak. For this purpose, test calculations for different distances to the boundaries were made.

To elucidate the role of different heat release mechanisms in the SLSCW propagation process, the problem was analysed not only with the complete RGD model (1)–(9), which takes into account all types of heat exchange (heat conductivity, convection, and radiative heat exchange, including reabsorption) and the motion of a medium, but by also using the following approximate models:
the radiative-conductive (RC) model in which the motion of a medium and the convective heat exchange were ignored;
the radiative gas-dynamic model of bulk emission (the RGDBE model) in which radiation reabsorption was ignored;
the radiative-conductive model of bulk emission (the RCBE model) in which radiation reabsorption and convective motion were ignored.

Moreover, modified optical models (MOMs) were used in the calculations. The modification consisted in the fact that the group absorption coefficient of the base optical model was multiplied by a factor A; i.e., if k_k is the group absorption coefficient for the kth energy group, then $k_k^{\mathrm{MOM}} = Ak_k$ is the group absorption coefficient for a MOM. The base optical model ($N_k = 10$) was developed by using the MONSTER computer system [21].

3. Experimental data of Klosterman and Byron [8]

In the experiments [8], a 500-kW gas-dynamic CO_2 laser was used, which produced laser radiation at 10.6 μm during ~ 5 ms. Plasma was produced by focusing CO_2 laser radiation onto Al or Ti targets. The laser beam diameter on a target was about 1 cm. The wave of laser radiation absorption, which was initially formed in target vapours rapidly changed to the wave of absorption in the ambient air, where its quasi-stationary propagation toward a laser beam was observed.

The process developed in time in the following way. First, the laser radiation power linearly increased (during the first 1.5 ms) up to its maximum value ($\sim 300 - 500$ kW). Approximately 0.75 ms after the beginning of the process, the appearance of emission from the surface of an irradiated target was observed, and a laser-supported combustion wave in target vapours was formed ~ 0.75 ms later. Then, stable lasing with a maximum radiation power was observed during 2–3 ms. This time range was best suited for measuring the SLSCW velocity because the time interval 1.5–2 ms long was characterised by a change of laser-supported combustion wave from target vapours to atmospheric air, and after that, the ionisation wave velocity was stabilised. During the last 3–5 ms, the laser radiation power nonmonotonically decreased, which caused a decrease in the SLSCW velocity.

The results of measurements of the SLSCW velocity in laser beams of different diameter, for laser radiation intensity varied in a wide range, are presented in Fig. 2.

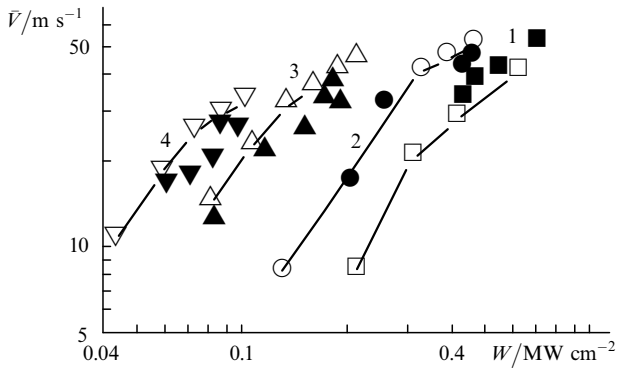

Figure 2. Dependences of the SLSCW velocity on the laser radiation intensity for laser beam diameters of 5 (1), 10 (2), 15.5 (3), and 21 mm (4) in the experiment [8] (bold symbols) and the numerical calculation made in the present paper (empty symbols).

4. Calculation of SLSCW velocities

Calculations were made for four laser beam diameters $d = 2R_L = 5$, 10, 15.5, and 21 mm. The laser radiation power P_L was varied in the 50 – 350-kW range, which gave the laser radiation intensity W in a range of $\sim 0.04 - 0.8$ MW cm^{-2}, as in the experiments [8]. The factor n describing the intensity distribution in the radial section of a laser beam was taken equal to 3.

The calculations used the same scheme for determining the SLSCW velocity as the one used in the experiments. For this purpose, the position of the SLSCW front boundary (facing the laser beam) in the laboratory coordinate system at different moments of time was determined. The SLSCW velocity was measured on the path $x = 4 - 9$ cm, where the position of the SLSCW at 20 points was determined. Typical examples of $(x - t)$ diagrams describing the motion of the leading front of the SLSCW are presented in Fig. 3.

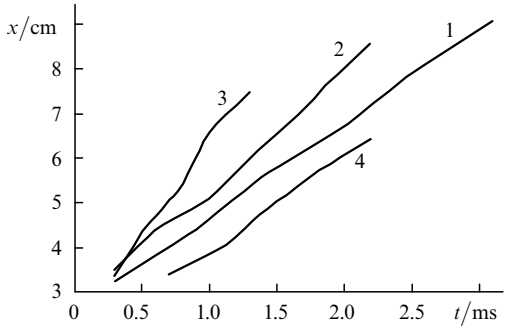

Figure 3. Time dependences of the SLSCW wavefront coordinate ($x - t$ diagram) for laser beam radii $R_L = 10.5$ (1), 7.75 (2), 5 (3), and 2.5 cm (4) for laser radiation powers $P_L = 200$ (**1**, **2**), 250 (3), and 60 kW (4) obtained in the calculations based on the RGD model.

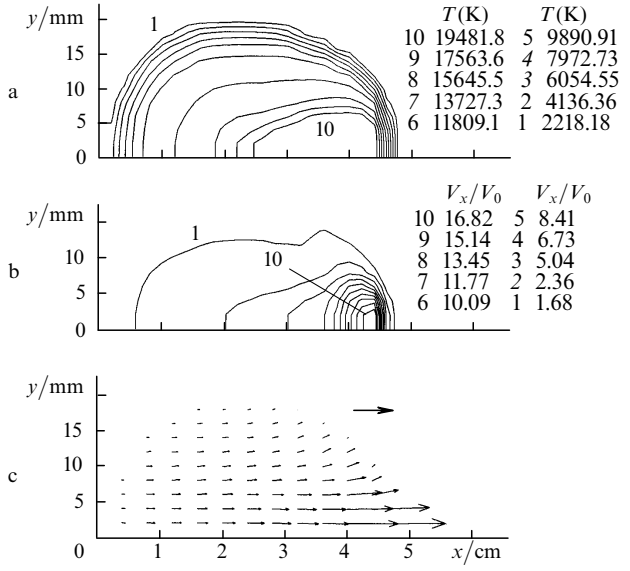

Figure 4. Structure of the SLSCW (RGD model) 0.986 ms after the origin of the process for a laser power of 200 kW and a laser beam radius of 1.05 cm. (a) Temperature distribution (the laser beam is directed from the right to the left), (b) axial-velocity distribution, and (c) the vector velocity field (the scale arrow corresponds to 10 m s^{-1}); $V_0 = 31.3$ cm s^{-1} is the characteristic velocity of thermal gravitational convection, which corresponds to a 1-cm scale.

The calculated data are analysed in this paper only for one of the versions corresponding to $d = 21$ mm and $P_L = 200$ kW. The basic conclusions are valid for the rest of the versions as well. Figs 4 – 6 present the distributions of temperature and gas-dynamic parameters in the SLSCW at three successive moments of time $t = 0.986$, 1.885, and 2.667 ms. They were obtained by using the basic RGD model.

Fig. 7 presents the results of calculations obtained for this version by using different heat exchange models. Among four calculation models using the base optical model, the RGD and RC models give almost identical results, which agree well with the experimental data (see Fig. 2). The models in which the assumption is made that the ray energy is emitted

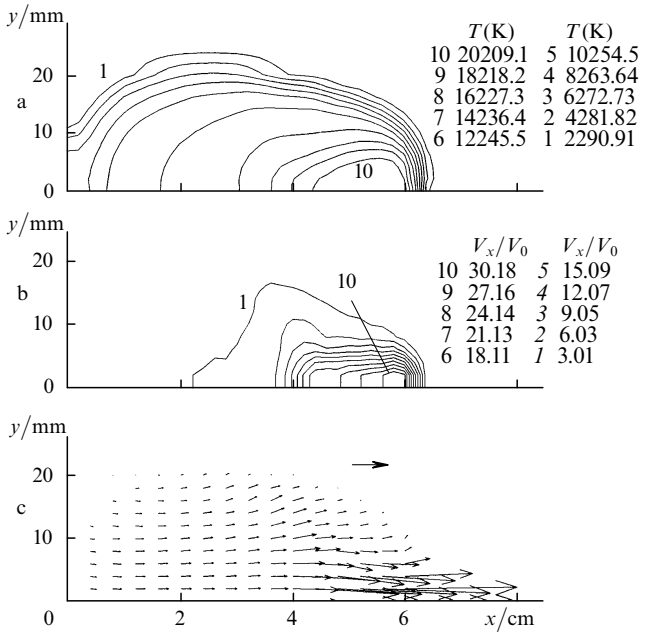

Figure 5. Structure of the SLSCW (RGD model) 1.885 ms after the origin of the process (the notation is the same as in Fig. 4).

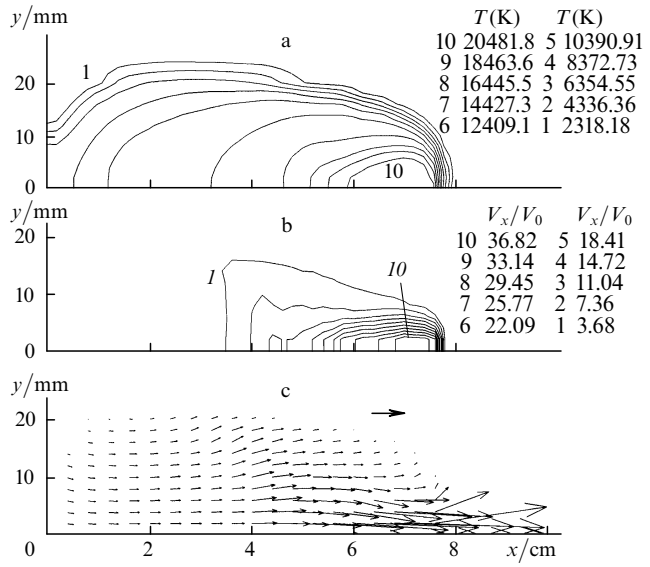

Figure 6. Structure of the SLSCW (RGD model) 2.667 ms after the origin of the process (the notation is the same as in Fig. 4).

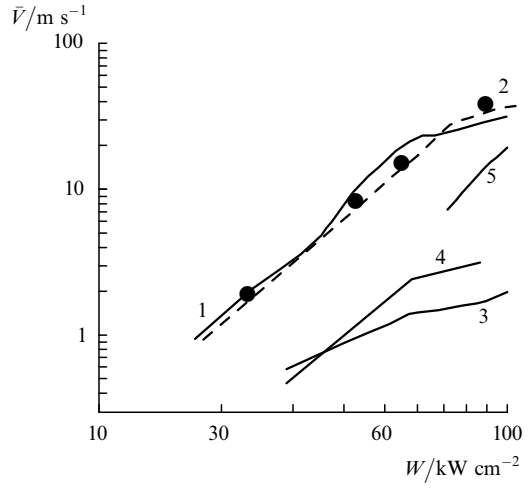

Figure 7. Velocities of laser-supported combustion waves calculated for a laser beam 10.5 mm in diameter by using the RGD model (1), the RC model (2), the RGDBE model (3), the RCBE model (4), and the RGD model (5) with a MOM ($k_{\mathrm{MOM}} = 10k$) (5).

from the bulk (the RGDBE and RCBE models) also give close results, but they are understated with respect to the experimental data by a factor of more than ten.

It is worth noting that the gas-dynamic processes have virtually no effect on the wave velocity under the given conditions. It is pertinent to note that this does not mean that the SLSCWs move in an immobile air. One can see from Figs 4 – 6 that a gas-dynamic field with a rather high velocity of gas motion is formed in its neighbourhood.

The fact that the velocity of the SLSCW in the case under consideration is governed by the heat radiation absorption ahead of its front suggests that the optical properties of low-temperature plasma used in the calculations should have a noticeable effect on the calculated SLSCW velocity. This may account for the disagreement between the calculated [9] and the experimental [8] data presented in Fig. 1. This is also supported by the calculations given by the RGD model with a MOM, where understated values of velocity $\bar{V}$ were obtained, which coincide with the results of the calculations [9].

5. Conclusions

The systematic numerical study of the temperature and gas-dynamic structure of SLSCWs under the conditions of experiments [8] showed that the propagation of SLSCWs is governed by reabsorption of heat radiation ahead of the wave front; i.e., the waves travel in the radiation regime. The effect of gas dynamics of the process on the wave velocity is insignificant, and the gas-dynamic structure does not have time to be developed.

Acknowledgements. This work was supported by the Russian Foundation for Basic Research, Grant No. 98-02-17728.

References

1. Bunkin V F, Konov V I, Prokhorov A M, Fedorov V B Pis'ma Zh. Eksp. Teor. Fiz. **9** 609 (1969) [JETP Lett. **9**(1969)]
2. Bufetov I A, Prokhorov A M, Fedorov V B, et al. Tr. Inst. Obshch. Fiz. Akad. Nauk SSSR **10** 3 (1988)
3. Raĭzer Yu P Pis'ma Zh. Eksp. Teor. Fiz. **11** 195 (1970) [JETP Lett. **11** 120 (1970)]
4. Generalov N A, Zimakov V P, Kozlov G I, et al. Pis'ma Zh. Eksp. Teor. Fiz. **11** 447 (1970) [JETP Lett. **11** 302 (1970)]
5. Raĭzer Yu P Zh. Eksp. Teor. Fiz. **58** 2127 (1970)
6. Landau L D, Lifshitz E M Fluid Mechanics (2nd ed.) (Oxford: Pergamon Press, 1987)
7. Gus'kov K G, Raizer Yu P, Surzhikov S T Kvantovaya Elektron. (Moscow) **17** 937 (1990) [Sov. J. Quantum Electron. **20** 860 (1990)]
8. Klosterman E L, Byron S R J. Appl. Phys. **45** 4751 (1974)
9. Jackson J P, Nielsen P E AIAA J. **12** 1498 (1974)
10. Conrad R, Raizer Yu P, Surzhikov S T AIAA J. **34** 1584 (1996)
11. Kozik E A, Loseva T V, Nemchinov I V, et al. Kvantovaya Elektron. (Moscow) **5** 2138 (1978) [Sov. J. Quantum Electron. **8** 1206 (1978)]
12. Raĭzer Yu P, Surzhikov S T Kvantovaya Elektron. (Moscow) **11** 2301 (1984) [Sov. J. Quantum Electron. **14** 1526 (1984)]
13. Raizer Yu P, Surzhikov S T Teplofiz. Vys. Temp. **23** 29 (1985)
14. Raĭzer Yu P, Silant'ev A Yu, Surzhikov S T Teplofiz. Vys. Temp. **25** 454 (1987)
15. Surzhikov S T Matemat. Model. **2** (7), 85 (1990)
16. Loseva T V, Nemchinov I V Kvantovaya Elektron. (Moscow) **19** 250 (1992) [Quantum Electron. **22** 227 (1992)]
17. Demchenko V V, Loseva T V, Nemchinov I V Kvantovaya Elektron. (Moscow) **19** 257 (1992) [Quantum Electron. **22** 233 (1992)]
18. Loseva T V, Nemchinov I V Mekh. Zhidk. Gaza (5) 166 (1993)
19. Surzhikov S T Matemat. Model. **7** (6) 3 (1995)
20. Surzhikov S T Mekh. Zhidk. Gaza (3) 138 (1997)
21. Surzhikov S T Vychislitel'nyĭ Eksperiment v Postroenii Radiatsionnykh Modelei Mekhaniki Izluchayushchego Gaza (Calculation Experiment in the Construction of Radiative Models of Mechanics of an Emitting Gas) (Moscow: Nauka, 1992)